

Rashbons: Properties and their significance

Jayantha P. Vyasankere* and Vijay B. Shenoy†

Centre for Condensed Matter Theory, Department of Physics,
Indian Institute of Science, Bangalore 560 012, India

(Dated: August 24, 2011)

In presence of a synthetic non-Abelian gauge field that induces a Rashba like spin-orbit interaction, a collection of weakly interacting fermions undergoes a crossover from a BCS ground state to a BEC ground state when the strength of the gauge field is increased [Phys. Rev. B **84**, 014512 (2011)]. The BEC that is obtained at large gauge coupling strengths is a condensate of tightly bound bosonic fermion-pairs whose properties are solely determined by the Rashba gauge field – hence called rashbons. In this paper, we conduct a systematic study of the properties of rashbons and their dispersion. This study reveals a new qualitative aspect of the problem of interacting fermions in non-Abelian gauge fields, i. e., that the rashbon state induced by the gauge field for small centre of mass momenta of the fermions ceases to exist when this momentum exceeds a critical value which is of the order of the gauge coupling strength. The study allows us to estimate the transition temperature of the rashbon BEC, and suggests a route to enhance the exponentially small transition temperature of the system with a fixed weak attraction to the order of the Fermi temperature by tuning the strength of the non-Abelian gauge field. The nature of the rashbon dispersion, and in particular the absence of the rashbon states at large momenta, suggests a regime of parameter space where the normal state of the system will be a dynamical mixture of uncondensed rashbons and unpaired helical fermions. Such a state should show many novel features including pseudogap physics.

PACS numbers: 03.75.Ss, 05.30.Fk, 67.85.Lm

I. INTRODUCTION

Cold atoms are a promising platform for quantum simulations. Controlled generation of synthetic gauge fields¹⁻³ has provided impetus to the realization of novel phases in cold atomic systems. The recent generation of synthetic non-Abelian gauge fields in ⁸⁷Rb atoms³ is a key step forward in this regard. While a uniform Abelian gauge field is merely equivalent to a galilean transformation, even a uniform non-Abelian gauge field nurtures interesting physics.³⁻⁵

The clue that a uniform non-Abelian gauge field crucially influences the physics of interacting fermions came from the study of bound states of two spin- $\frac{1}{2}$ fermions in its presence.⁶ The remarkable result found for spin- $\frac{1}{2}$ fermions in three spatial dimensions interacting via a *s*-wave contact interaction in the singlet channel is that high-symmetry non-Abelian gauge field configurations (GFCs) induce a two-body bound state for *any* scattering length however small and negative. The physics behind this unusual role of the non-Abelian gauge field that produces a generalized Rashba spin-orbit interaction, was explained by its effect on the infrared density of the states of the noninteracting two-particle spectrum. The non-Abelian gauge field drastically enhances the infrared density of states, and this serves to “amplify the attractive interactions”. A second most remarkable feature demonstrated in ref. [6] is that wave function of the bound state that emerges has a triplet content and associated spin-nematic structure similar to those found in liquid ³He.

The above study⁶ motivated the study of interacting fermions at a *finite* density in the presence of a non-

Abelian gauge field.⁷ At a finite density ρ ($\sim k_F^3$, k_F is the Fermi momentum), the physics of interacting fermions in a synthetic non-Abelian gauge field is determined by two dimensionless scales. The first scale is associated with the size of the interactions $-1/k_F a_s$ where a_s is the *s*-wave scattering length, and the second one, $\frac{\lambda}{k_F}$, is determined by the non-Abelian gauge coupling strength λ . For small negative scattering lengths ($-1/k_F a_s \gg 1$), the ground state in the absence of the gauge field is a BCS superfluid state with large overlapping pairs. The key result first demonstrated in ref. [7] is that at a *fixed scattering length*, even if small and negative, the non-Abelian gauge field induces a crossover of the ground state from the just discussed BCS superfluid state to a new type of BEC state. The BEC state that emerges is a condensate of a collection of bosons which are tightly bound pairs of fermions. Remarkably, at large gauge couplings $\lambda/k_F \gg 1$, the nature of the bosons that make up the condensate is determined *solely by the gauge field* and is not influenced by the scattering length (so long as it is non-zero), or by the density of particles. In other words, the BEC state that is attained in the $\lambda/k_F \gg 1$ regime at a fixed scattering length does not depend on the value of the scattering length, i. e., the BEC is a condensate of a novel bosonic paired state of fermions determined by the non-Abelian gauge field. These bosons were called as “rashbons” since their properties are determined solely by the generalized Rashba spin-orbit coupling produced by the gauge field. As shown in ref. [7], rashbon is the bound state of two fermions at infinite scattering length (resonance) in the presence the non-Abelian gauge field. The crossover from the BCS state to the “rashbon BEC” state (RBEC) induced by the gauge field at a

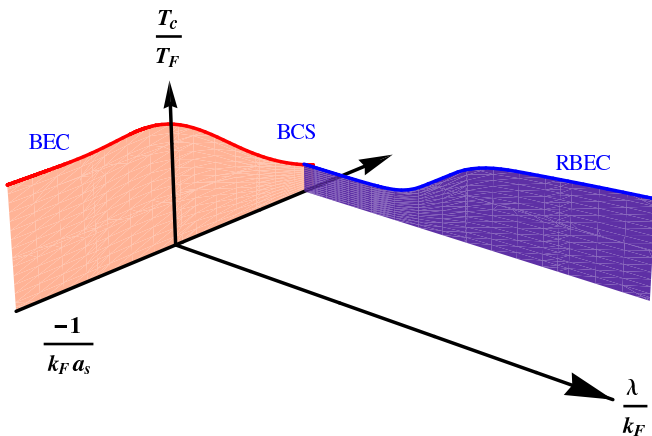


FIG. 1. BCS-RBEC crossover induced by a non-Abelian gauge field. Here, a_s is the s -wave scattering length, k_F is the Fermi momentum determined by the density, T_F is the Fermi temperature ($= k_F^2/2$), T is the temperature λ is the strength of the gauge coupling. The solid red line is the transition temperature of the superfluid phase (shaded in light red) obtained in ref. 18 using the Nozières-Schmitt-Rink theory¹⁹. The solid blue curve is based on the estimate presented in this work. The figure reveals the qualitative features of the full “phase diagram” in the $T - a_s - \lambda$ space. (Figure courtesy: Sudeep Kumar Ghosh)

fixed scattering length is to be contrasted with the traditional BCS-BEC crossover^{8–11} by tuning the scattering length^{12–14}, but with no gauge field. Gong et al.¹⁵ have investigated the crossover including the effects of a Zeeman field along with a non-Abelian gauge field. Certain properties of rashbons in the EO gauge field (explained later) have been investigated in references [16] and [17].

It was shown in ref. [7] that the Fermi surface of the non-interacting system (with $a_s = 0$) in presence of the non-Abelian gauge field undergoes a change in topology at a critical gauge coupling strength λ_T (of order k_F). For weak attractions ($-1/k_F a_s \gg 1$), the regime of the gauge coupling strengths where the crossover from the BCS state to the RBEC state takes place coincides with the regime where the bare Fermi surface undergoes the topology change. The properties of the superfluid state (such as the transition temperature) for $\lambda \gtrsim \lambda_T$ was argued to be primarily determined by the properties of the constituent anisotropic rashbons (see Sect. V of ref. [7]). It is, therefore, necessary and fruitful to undertake a detailed study of the properties of rashbons and their dispersion, and this is the aim of this paper.

In this paper, we study the properties of rashbons and their dependence on the nature of the non-Abelian gauge field, i.e., we obtain properties of rashbons for the most interesting gauge field configurations. This study entails a study of the anisotropic rashbon dispersion, i. e., determination of its energy as a function of its momentum by the study of the two-body problem in a non-Abelian gauge field with a resonant scattering length ($1/\lambda a_s = 0$). In addition to the determination of the properties of rash-

bons, we report here a new qualitative result. It is shown that *when the momentum of a rashbon exceeds a critical value which is of the order of the gauge coupling strength, it ceases to exist*. Stated otherwise, when the center of mass momentum of the two fermions that make up the bound pair exceeds a value of order of the gauge coupling strength, the bound state disappears. To uncover the physics behind this result, the two-fermion problem in a gauge field is investigated in detail for a range scattering of lengths and centre of mass momenta. The study reveals a hitherto unknown feature of the non-Abelian gauge fields: while the non-Abelian gauge field acts as attractive interaction amplifiers for fermions with centre of mass momenta q much smaller than the gauge field strength ($q \ll \lambda$), the gauge field *suppresses the formation of bound states of fermions with large centre of mass momenta* ($q \gtrsim \lambda$). In fact, it is demonstrated here that when $q \gtrsim \lambda$, a *positive* scattering length (very strong attraction) is necessary to induce a bound state of the two fermions, quite contrary to $q \ll \lambda$ where a bound state exists (essentially) for any scattering length.

The results we report here have two significant outcomes. (1) A full qualitative picture of the BCS-BEC crossover scenario in the presence of a non-Abelian gauge field is obtained (see Fig. 1) based on the results reported here. Most notably, it is shown that the transition temperatures of a system of fermions with a very weak attraction can be enhanced to the order of the Fermi temperature (determined by the density) by the application of a non-Abelian gauge field. (2) Our two body results at large centre of mass momenta suggest that the normal state of the fermion system in non-Abelian gauge field will be a “dynamic mixture” of rashbons and interacting helical fermions. These could therefore show many novel features such as pronounced pseudogap characteristics (see ref. 20 and references therein).

The next section, II, contains the preliminaries which includes the formulation of the problem. Sec. III contains a report on the properties of rashbons, and this is followed by sec. IV which discusses the bound state of two fermions for arbitrary centre of mass momentum and scattering length for specific high symmetry gauge fields. The importance of the results obtained here is discussed in sec. V, and the paper is concluded with a summary in sec. VI.

II. PRELIMINARIES

The Hamiltonian of the fermions moving in a uniform non-Abelian gauge field that leads to a generalized Rashba spin-orbit interaction is²¹

$$\mathcal{H}_R = \int d^3\mathbf{r} \Psi^\dagger(\mathbf{r}) \left(\frac{\mathbf{p}^2}{2} \mathbf{1} - \mathbf{p}_\lambda \cdot \boldsymbol{\tau} \right) \Psi(\mathbf{r}), \quad (1)$$

where $\Psi(\mathbf{r}) = \{\psi_\sigma(\mathbf{r})\}$, $\sigma = \uparrow, \downarrow$ are fermion operators, \mathbf{p} is the momentum, $\mathbf{1}$ is the $SU(2)$ identity, τ^μ ($\mu = x, y, z$) are Pauli matrices, $\mathbf{p}_\lambda = \sum_i p_i \lambda_i \mathbf{e}_i$, \mathbf{e}_i 's are the unit

vectors in the i -th direction, $i = x, y, z$. The vector $\boldsymbol{\lambda} = \lambda \hat{\boldsymbol{\lambda}} = \sum_i \lambda_i \mathbf{e}_i$ describes a gauge-field configuration (GFC) space; we refer $\lambda = |\boldsymbol{\lambda}|$ as the gauge-coupling strength. Throughout, we have set the mass of the fermions (m_F), Planck constant (\hbar) and Boltzmann constant (k_B) to unity.

In this paper we specialize to $\boldsymbol{\lambda} = (\lambda_l, \lambda_l, \lambda_r)$ as this contains all the experimentally interesting high-symmetry GFCs. Moreover, it is shown in Ref. [6 and 7], that this set of gauge fields captures all the qualitative physics of the full GFC space. Specific high symmetry GFCs are obtained for particular values of λ_r and λ_l : $\lambda_r = 0$ corresponds to extreme oblate (EO) GFC; $\lambda_r = \lambda_l$ corresponds to spherical (S) GFC, and $\lambda_l = 0$ corresponds to extreme prolate (EP) GFC.

The interaction between the fermions is described by a contact attraction in the singlet channel

$$\mathcal{H}_v = v \int d^3\mathbf{r} \psi_{\uparrow}^{\dagger}(\mathbf{r}) \psi_{\downarrow}^{\dagger}(\mathbf{r}) \psi_{\downarrow}(\mathbf{r}) \psi_{\uparrow}(\mathbf{r}). \quad (2)$$

Ultraviolet regularization²² of the theory described by $\mathcal{H} = \mathcal{H}_R + \mathcal{H}_v$ is achieved by exchanging the bare interaction v for the scattering length a_s via $\frac{1}{v} + \Lambda = \frac{1}{4\pi a_s}$, where Λ is the ultraviolet momentum cutoff. Note that a_s is the s -wave scattering length in free vacuum, i. e., when the gauge field is absent ($\lambda = 0$).

The one-particle states of \mathcal{H}_R are described by the quantum numbers of momentum \mathbf{k} and helicity α (which takes on values \pm): $|\mathbf{k}\alpha\rangle = |\mathbf{k}\rangle \otimes |\alpha\hat{\mathbf{k}}_{\lambda}\rangle$. The one-particle dispersion is $\varepsilon_{\mathbf{k}\alpha} = \frac{k^2}{2} - \alpha|\mathbf{k}_{\lambda}|$, where \mathbf{k}_{λ} is defined analogously with \mathbf{p}_{λ} and $|\alpha\hat{\mathbf{k}}_{\lambda}\rangle$ is the spin-coherent state in the direction $\alpha\hat{\mathbf{k}}_{\lambda}$. The two-particle states of \mathcal{H} can be described using the basis states $|\mathbf{q}\mathbf{k}\alpha\beta\rangle = |(\frac{\mathbf{q}}{2} + \mathbf{k})\alpha\rangle \otimes |(\frac{\mathbf{q}}{2} - \mathbf{k})\beta\rangle$ where, $\mathbf{q} = \mathbf{k}_1 + \mathbf{k}_2$ is the center of mass momentum and $\mathbf{k} = (\mathbf{k}_1 - \mathbf{k}_2)/2$ is the relative momentum of two particles with momenta \mathbf{k}_1 and \mathbf{k}_2 . Note that \mathbf{q} is a good quantum number for the full Hamiltonian (\mathcal{H}). The non-interacting two-particle dispersion is $E_{\mathbf{q}\mathbf{k}\alpha\beta}^{free} = \varepsilon_{(\frac{\mathbf{q}}{2} + \mathbf{k})\alpha} + \varepsilon_{(\frac{\mathbf{q}}{2} - \mathbf{k})\beta}$. In the presence of interactions, bound states emerge as isolated poles of the T -matrix, and are roots of the equation

$$\frac{1}{4\pi a_s} = \frac{1}{V} \sum_{\mathbf{k}\alpha\beta} \left(\frac{|A_{\alpha\beta}^{\mathbf{q}}(\mathbf{k})|^2}{E(\mathbf{q}) - E_{\mathbf{q}\mathbf{k}\alpha\beta}^{free}} + \frac{1}{4k^2} \right) \quad (3)$$

where, $A_{\alpha\beta}^{\mathbf{q}}(\mathbf{k})$ is the singlet amplitude in $|\mathbf{q}\mathbf{k}\alpha\beta\rangle$, V is the volume, $E(\mathbf{q}) = E_{th}(\mathbf{q}) - E_b(\mathbf{q})$ is the energy of the bound state. Here $E_{th}(\mathbf{q})$ is the scattering threshold and $E_b(\mathbf{q})$ is the binding energy, both of which depend on \mathbf{q} as indicated.

In the absence of the gauge field ($\lambda = 0$), the bound state exists only for $a_s > 0$ and $E_b(\mathbf{q}) = -1/a_s^2$ is independent of \mathbf{q} . The threshold is $E_{th}(\mathbf{q}) = q^2/4$. Physically, this corresponds to the fact that a critical attraction is necessary in free vacuum ($\lambda = 0$) for the formation of the two-body bound state. As shown in ref. [6], state of

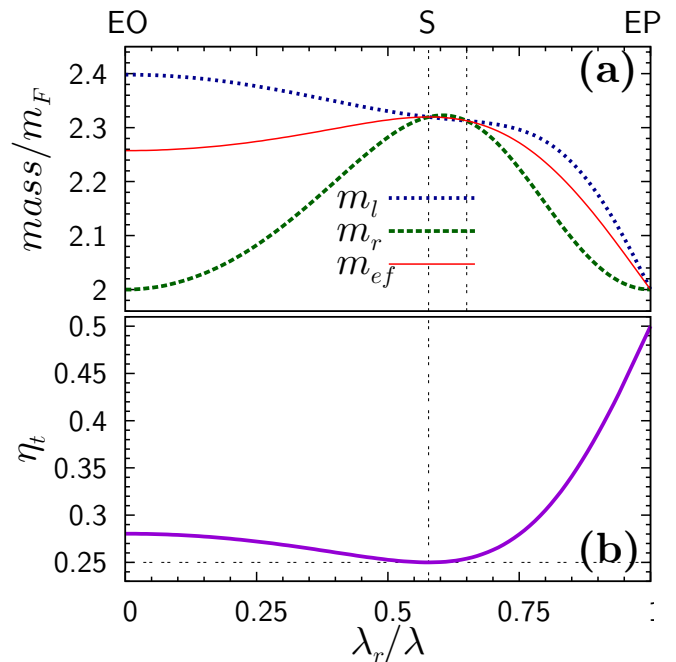


FIG. 2. (Color online) Rashbon properties for different GFCs. (a) In-plane, perpendicular and effective masses. (b) The triplet content of rashbons.

affairs change drastically in the presence of a non-Abelian gauge field. For $\mathbf{q} = 0$, the presence of the gauge field always reduces the critical attraction to form the bound state and in particular, for special high symmetry GFCs (e.g. $\boldsymbol{\lambda} = (\lambda_l, \lambda_l, \lambda_r)$ with $\lambda_r \leq \lambda_l$) two body bound state forms for any scattering length.⁶

III. PROPERTIES OF RASHBONS

The bound state that emerges in the presence of the gauge field when the scattering length is set to the resonant value $1/a_s = 0$ is the rashbon. As argued above, the binding energy of the rashbon state for all the GFCs considered here (except for the EP GFC) is positive. The energy of the rashbon state $E_R(\mathbf{q} = 0)$ determines the chemical potential of the RBEC. Other properties of the RBEC are determined by the rashbon dispersion $E_R(\mathbf{q})$, and in particular the transition temperature will be determined by the mass of the rashbons.

The curvature of the rashbon dispersion $E_R(\mathbf{q})$ at $\mathbf{q} = \mathbf{0}$ defines the effective low-energy inverse mass of rashbons. The dispersion is in general anisotropic and the inverse mass is, in general, a tensor. However, due to their symmetry, for the GFCs considered in this paper ($\boldsymbol{\lambda}$ of the form $(\lambda_l, \lambda_l, \lambda_r)$), $E_R(\mathbf{q}) = E_R(q_l, q_r)$, where q_l is the component of \mathbf{q} on the $x-y$ plane, and q_r is the component along \mathbf{e}_z . Thus, the inverse mass tensor is completely specified by its principal elements - in-plane inverse mass (m_l^{-1}) and the ‘‘perpendicular’’ inverse mass,

m_r^{-1} .

$$m_l^{-1} = \left. \frac{\partial^2 E_R(q_l, q_r)}{\partial q_l^2} \right|_{q=0}, \quad m_r^{-1} = \left. \frac{\partial^2 E_R(q_l, q_r)}{\partial q_r^2} \right|_{q=0} \quad (4)$$

An effective mass m_{ef} defined as

$$m_{ef} = \sqrt[3]{(m_r m_l^2)} \quad (5)$$

is useful in the discussions that follow.

In addition to the anisotropy in their orbital motion, rashbons are intrinsically anisotropic particles. Their pair-wave function has both a singlet and triplet component; the weight of the pair wave function in the triplet sector η_t is the triplet content. The triplet component is time reversal symmetric, but does not have the spin rotational symmetry – it is therefore a spin nematic. Keeping this interesting aspect in mind, we shall also investigate and report the triplet content of rashbons, and its dependence on the gauge field.

Before presenting the results we make a general observation. The threshold energy (E_{th}) becomes increasingly flat as a function of \mathbf{q} in the small \mathbf{q}/λ regime as one approaches spherical gauge field in the GFC space. In fact, for the spherical GFC, it is exactly constant in the small \mathbf{q}/λ regime (see Fig. 3). The mass is therefore determined entirely by the variation of the binding energy with \mathbf{q} (this may be contrasted in free vacuum case discussed before). It is reasonable therefore to expect that the effective mass of rashbons is always greater than twice the bare fermion mass and for it to be the largest for the spherical GFC.

Fig. 2 (a) shows the in-plane, perpendicular, and effective masses for different GFCs. Rashbons emerging from spherical GFCs have the highest m_{ef} and that from EP GFCs have the least. It is interesting to note that apart from the spherical GFC, there is yet another GFC ($\lambda_r \approx 0.65\lambda$ - see fig. 2 (a)) where the low energy dispersion is isotropic, i. e., rashbon has a scalar mass. The triplet content is shown in fig. 2 (b) for different GFCs. η_t is minimum (1/4) for spherical GFC and maximum (1/2) for EP GFC.

A detailed study of rashbon dispersion as a function of its momentum \mathbf{q} (centre of mass momentum of the fermions that make up the rashbon) revealed a hitherto unreported and rather unexpected feature. The full rashbon dispersion as a function of \mathbf{q} for the spherical (S) GFC is shown in Fig. 3. The rashbon energy increases with increasing q and eventually for $q/\lambda \gtrsim 1.3$, there is no two body bound state! This curious result motivated us to perform a more detailed investigation of the dispersion of the bound fermions (bosons) at arbitrary scattering lengths (away from resonance which corresponds to rashbons), in order to uncover the physics behind this phenomenon. This study, conducted for specific high symmetry GFCs, is presented in the next section.

IV. DISPERSION OF BOSONS AT ARBITRARY SCATTERING LENGTHS FOR SPECIFIC GFCs

In this section we investigate the dispersion of the bosonic bound state of two fermions at arbitrary scattering length. Results of the boson dispersion obtained by solving eqn. (3) will be presented for the S and EO GFCs.

A. Spherical GFC

Spherical (S) GFC corresponds to $\lambda_r = \lambda_l$ and hence produces an isotropic boson dispersion as discussed before. The boson dispersion depends only on $q = |\mathbf{q}|$. Solving eqn. (3), the boson dispersion obtained for various scattering lengths is as shown in fig. 3(a). The key features of this spectrum are the following. For *any scattering length, however large and positive*, there exists a critical center of mass momentum q_c such that when $q > q_c$ the bound state ceases to exist.

This is best understood by fixing attention on a particular momentum q . When the momentum is “small”, there is a bound state for *any attraction*. This is in fact the case for all $q < q_o$, where $q_o = 2\frac{\lambda}{\sqrt{3}}$. For $q > q_o$, a critical attraction described by a nonzero scattering length a_{sc} is necessary for the formation of a bound state. For $q = q_o^+$, the critical scattering length is $a_{sc} = -\frac{2\sqrt{3}}{\lambda}$. On increasing q , a stronger attractive interaction is required to produce a bound state and when q reaches $\sim \frac{4\lambda}{3}$, a resonant attraction is necessary to produce a bound state. For $q \gtrsim \frac{4\lambda}{3}$, a very strong attractive interaction described by a small positive scattering length is necessary to produce a bound state. In fact, for $q \gg \lambda$, the critical scattering length scales as $a_{sc} \sim \sqrt{\frac{1}{\lambda q}}$. The dependence of a_{sc} on the centre of mass momentum is shown in Fig. 3(b).

How do we understand these results? Here the $\varepsilon_0 - \gamma$ model introduced in Ref. 6 comes to our rescue. The model states that if the infrared density of states $g_s(\varepsilon) \sim \varepsilon^\gamma$ for $0 \leq \varepsilon \leq \varepsilon_0$, where ε is the energy measured from the scattering threshold, then the critical scattering length is given by $\sqrt{\varepsilon_0} a_{sc} \propto \gamma \Theta(\gamma)/(2\gamma - 1)$, where Θ is the unit step function. Note that for $\gamma < 0$, the critical scattering length vanishes.

It is evident that there is a drastic change in the infrared density of states at $q = q_o$. In fact, this special momentum q_o is such that the threshold energy corresponds to that state where the relative momentum \mathbf{k} between the pair of fermions vanishes. Clearly, for $q < q_o$, there are many degenerate \mathbf{k} states that produce a nonzero density of states at the threshold. In fact, when $q = 0$, the density of states diverges as $1/\sqrt{\varepsilon}$, i.e., $\gamma = -1/2$. For $q < q_o$, there is still a finite density of states at the threshold with an effective $\gamma < 0$. Thus the critical scattering length, as given by the $\varepsilon_0 - \gamma$ model, vanishes. Let us turn our attention to what happens for $q \gg \lambda$. From eqn. (3) it is evident that the density of states $g_s(\varepsilon)$ has

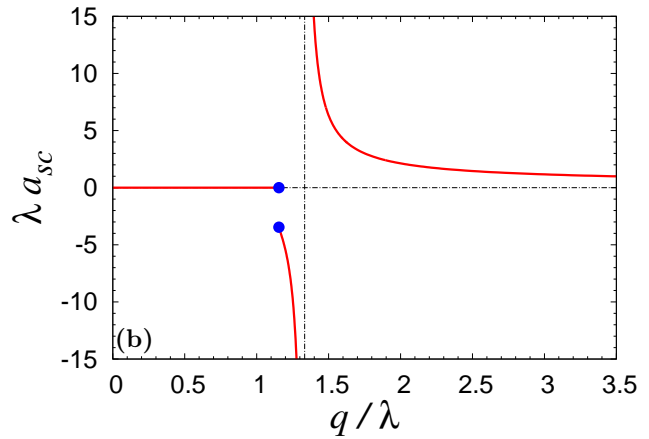
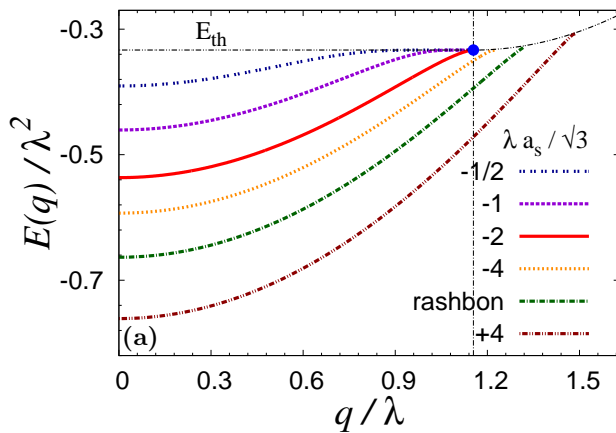


FIG. 3. (Color online) (a) The boson dispersion for various scattering lengths in spherical GFC. Note that for any given scattering length, the bound state disappears after some critical momentum. (b) Critical scattering length (a_{sc}) as a function of momentum. a_{sc} goes as $1/\sqrt{q}$ in the large q/λ limit.

the contributions from the $++$, $--$, $+-$ and $-+$ channels. It can be shown that in the regime $q \gg \lambda$, of the $++$ channel has a density of states that has $\varepsilon^{3/2}$ behaviour. The $+-$ and $-+$ channels have a higher threshold which is λq larger than the threshold of the $++$ channel; the density of states of the $+-/-+$ channels goes as $\sqrt{\varepsilon}$ form this higher threshold. These arguments provide an estimate of $\varepsilon_0 \approx q\lambda$. The result on the critical scattering length is then $a_{sc} \sim \frac{1}{\sqrt{q}}$, precisely as obtained from the full numerical solution shown in Fig. 3(b).

As a by product of the analysis of the boson dispersion, we were able to obtain an analytical expression for the mass of bosons (which is isotropic in this case)

$$\frac{m_B}{m_F} = \frac{6E(\mathbf{0})^{3/2}}{7E(\mathbf{0})^{3/2} + 2\sqrt{E(\mathbf{0})\lambda^2 - 4\left(E(\mathbf{0}) + \frac{\lambda^2}{3}\right)^{3/2}}, \quad (6)$$

where,

$$E(\mathbf{0}) = -\frac{\lambda^2}{3} - \frac{1}{4} \left(\frac{1}{a_s} + \sqrt{\frac{1}{a_s^2} + \frac{4\lambda^2}{3}} \right)^2 \quad (7)$$

At a given λ , as expected, mass for a small positive scattering length $a_s > 0$ is twice the fermion mass. Mass at resonance is the rashbon mass which is equal to $= \frac{3}{7}(4 + \sqrt{2})m_F \approx 2.32m_F$. Interestingly, the value of m_B/m_F for a small negative scattering length limit is (integer) 6.

B. Extreme oblate GFC

Extreme oblate (EO) GFC corresponds to $\lambda_r = 0$ with $\lambda_l = \frac{\lambda}{\sqrt{2}}$. It can be easily shown that for this GFC, $E(q_l, q_r) = E(q_l, 0) + \frac{q_r^2}{2}$. Thus, the two-body dispersion

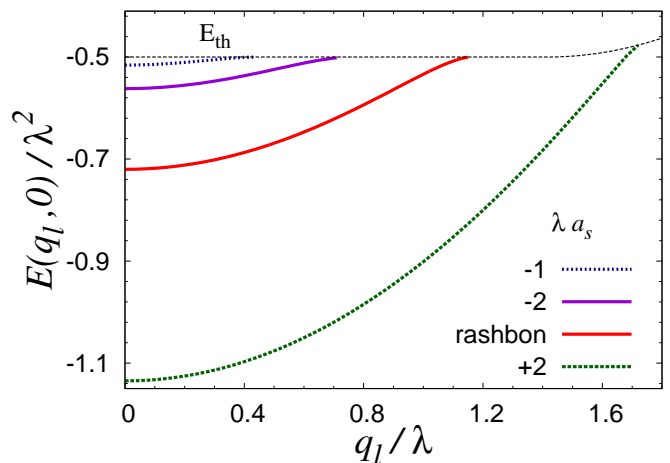


FIG. 4. (Color online) The boson dispersion for various scattering lengths in extreme oblate GFC. Just as in S GFC (see Fig. 3), for any given scattering length, the bound state disappears after some critical q_l .

as a function of q_l provide all the nontrivial features of the two-body problem arising from this gauge field.

Fig. 4 shows the boson dispersion for various scattering lengths. Remarkably, we find that the dispersion has very similar features as found for the spherical GFC, i.e., for any given scattering length there is a q_c such that for $q > q_c$, the two-body bound state ceases to exist. Clearly, this is a generic feature of the boson (bound fermion-pair) dispersion in a gauge field.

For this GFC, m_r is just twice the fermion mass. The in-plane mass (m_l) extracted from the two-body dispersion is shown in fig. 5. m_l for small positive scattering length is again twice the fermion mass. The resonance value which corresponds to rashbon is $m_l \simeq 2.4m_F$. This result agrees with refs. [16 and 17]. It is again interesting to note that value of m_l/m_F in the deep BCS limit

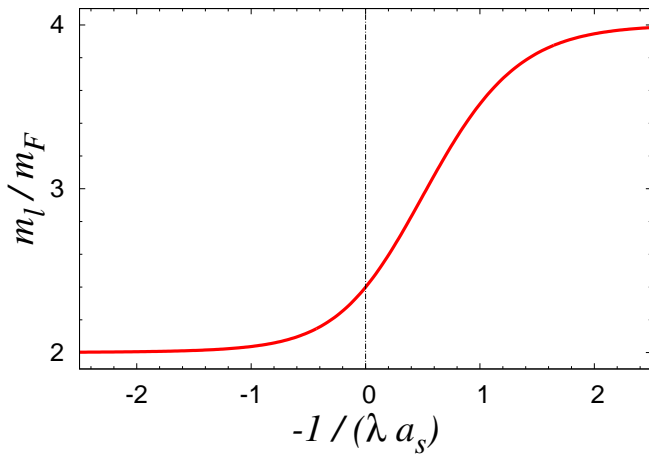


FIG. 5. (Color online) In-plane mass of tightly bound fermion pairs in the rashbon BEC side in presence of an extreme oblate GFC.

is (integer) 4.

C. Discussion

The analysis of the dispersion of the boson (bound-state of two fermions obtained in a gauge field) reveals that the boson ceases to exist when the momentum of the boson exceeds a critical value. For the case of rashbons (bosons obtained at resonance scattering length), the critical momentum is of the order of the strength of the gauge field.

The analysis presented here shows that this is again because of the influence of the gauge field in altering of the infrared density of states. When the momentum is smaller than the magnitude of the gauge coupling, the gauge field works to *enhance* the infrared density of states. On the other hand, for large momenta, the gauge field has the opposite effect, i. e., it *depletes* the infrared density of states.

V. SIGNIFICANCE OF THE RESULTS

The above results allow us to infer many key aspects of the physics of interacting fermions in the presence of a non-Abelian gauge field.

First, these results allow us to estimate the transition temperature. For large gauge couplings, the transition temperature as noted above will be determined by the mass of the rashbons. We have argued (and demonstrated) that the mass of the rashbons is always greater than twice the fermion mass. Thus the transition temperature of RBEC will always be less than that of the usual BEC of bound pairs of fermions obtained in the absence of the gauge field by tuning the scattering length to small positive values.

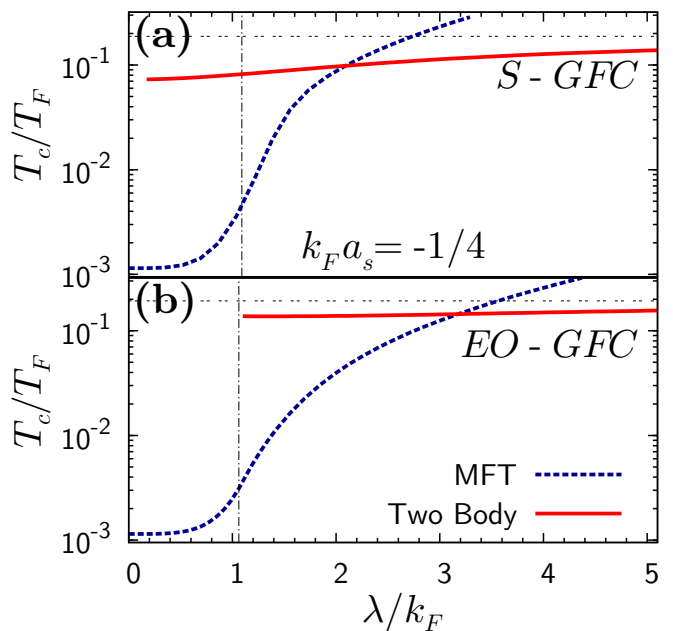


FIG. 6. (Color online) Estimate of transition temperature in spherical and extreme oblate GFCs as a function of the gauge coupling strength which takes the regular BCS state to a rashbon BEC. T_c in the small λ/k_F limit is obtained from mean field theory (analytical approximation is shown in the text). T_c in the large λ/k_F limit is obtained from the condensation temperature of the tightly bound pairs of fermions (analytical form for the S GFC can be obtained from eqn. (6) and eqn. (8)). Horizontal dashed line corresponds to rashbon T_c . Vertical line indicates the gauge coupling corresponding to the Fermi surface topology transition⁷.

However, there is something remarkable that a synthetic non Abelian gauge field can achieve. Consider a system with a weak attraction (small negative scattering length). In the absence of the gauge field, the transition temperature in the BCS superfluid state is exponentially small in the scattering length. Interestingly, the transition temperature can be brought to the order of Fermi temperature by increasing the magnitude of the gauge field strength (keeping the weak attraction, small negative scattering length, fixed).

While T_c in the BCS regime is determined by the pairing amplitude (Δ), in the BEC regime it is determined by the condensation temperature of the emergent rashbons.¹⁹

The mean field estimate of the former (i.e. for small $k_F|a_s|$, $a_s < 0$ and small λ/k_F) is obtained by simultaneously solving $-1/(4\pi a_s) = \frac{1}{2V} \sum_{\mathbf{k}\alpha} \left(\frac{\tanh \frac{\xi_{\mathbf{k}\alpha}}{2T_c}}{2\xi_{\mathbf{k}\alpha}} - \frac{1}{k^2} \right)$ and the number equation, $\rho = \frac{1}{V} \sum_{\mathbf{k}\alpha} 1 / \left(\exp \left(\frac{\xi_{\mathbf{k}\alpha}}{T_c} \right) + 1 \right)$, where $\xi_{\mathbf{k}\alpha} = \varepsilon_{\mathbf{k}\alpha} - \mu$. In this limit, the chemical potential at T_c is almost equal to that of the noninteracting one at zero temperature. i.e., $\mu(T_c, a_s, \lambda) \approx \mu(0, 0^-, \lambda)$, and $\Delta_{(T=0)}/T_c \approx \pi/e^\gamma$ where⁷ $\Delta_{(T=0)}$ is the pairing am-

plitude at zero temperature and γ is Euler's constant (≈ 0.577).

The T_c on the RBEC side can be extracted from the effective mass (m_{ef}) as condensation temperature of the bosonic pairs :

$$\frac{T_c}{T_F} = \left(\frac{16}{9\pi(\zeta(3/2))^2} \right)^{1/3} \frac{1}{m_{ef}}, \quad (\text{rashbon BEC}) \quad (8)$$

where we recall that $m_{ef} = (m_r m_l^2)^{1/3}$. Using the information of mass given earlier (eqn. (6) for S GFC and fig. 5 for EO GFC) one can obtain T_c in this regime as a function of λa_s in S and EO GFCs. In particular, rashbon T_c in S case is $\approx 0.188T_F$ and in EO case it is $\approx 0.193T_F$. The rashbon T_c can be obtained for various GFCs, using m_{ef} shown in fig. 2 (a). Since, among all GFCs, the rashbon mass corresponding to S GFC is the largest, it also corresponds to condensate with the smallest T_c .

The results obtained in both BCS and RBEC limits for $k_F a_s = -1/4$ in S and EO GFCs are shown in fig. 6. We can see, as advertised, that T_c has increased by two orders of magnitude with increasing gauge coupling strength λ . These considerations also allow us to infer an overall qualitative ‘‘phase diagram’’ in the $T - a_s - \lambda$ space as shown in Fig. 1.

What is the nature of the system above T_c ? There is a regime in the parameter space shown in Fig. 1, where the normal state can be quite interesting. Consider for example $\lambda \approx 1.5k_F$. The ground state will be ‘‘very bosonic’’ i. e., a condensate of rashbons in the zero momentum state. On heating the system above the transition temperature $\lesssim T_F$, the system becomes normal. Rashbons are excited to higher momenta states, and eventually break up into the constituent fermions since there is no bound state at higher momenta. There, should, therefore be a temperature range where the system is a dynamical mixture of uncondensed rashbons and high energy helical fermions – a state that should show many novel features such as, among other things, a pseudogap.

VI. SUMMARY

The new results of this paper are:

1. A systematic enumeration of the properties of rashbons, including closed form analytical formulae, for various gauge field configurations.
2. A detailed study of the rashbon (boson) dispersion, which results in a new qualitative observation. Although a zero centre of mass momentum bound state exists for any scattering length for many GFCs, the bound state vanishes when the centre of mass momentum exceeds a critical value. Thus, although the gauge field acts to promote bound state formation for small momenta, it acts oppositely, i. e., inhibits bound state formation for large momenta. We provide a detailed explanation of the physics behind the phonemon.

These results allow us to make two important inferences.

1. For a fixed weak attractive interaction, the exponentially small transition temperature of a BCS superfluid can be enhanced by orders of magnitude to the order the Fermi temperature of the system by increasing the magnitude of the gauge coupling.
2. There is a regime of $T - a_s - \lambda$ parameter space where the normal phase of the system will have novel features.

We hope that these results will stimulate further experimental and theoretical studies on this topic.

Acknowledgements J.V. acknowledges support from CSIR, India via a JRF grant. V.B.S. is grateful to DST, India (Ramanujan grant) and DAE, India (SRC grant) for generous support. We are grateful to Sudeep Kumar Ghosh for providing us with Fig. 1.

* jayantha@physics.iisc.ernet.in

† shenoy@physics.iisc.ernet.in

¹ Y.-J. Lin, R. L. Compton, A. R. Perry, W. D. Phillips, J. V. Porto, and I. B. Spielman, Phys. Rev. Lett. **102**, 130401 (2009).

² Y.-J. Lin, R. L. Compton, K. Jimenez-Garcia, J. V. Porto, and I. B. Spielman, Nature **462**, 628 (2009).

³ Y.-J. Lin, K. Jimenez-Garcia, and I. B. Spielman, Nature **471**, 83 (2011).

⁴ T.-L. Ho and S. Zhang, (2010), arXiv:1007.0650.

⁵ C. Wang, C. Gao, C.-M. Jian, and H. Zhai, Phys. Rev. Lett. **105**, 160403 (2010).

⁶ J. P. Vyasankere and V. B. Shenoy, Phys. Rev. B **83**, 094515 (2011).

⁷ J. P. Vyasankere, S. Zhang, and V. B. Shenoy, Phys. Rev. B **84**, 014512 (2011).

⁸ D. M. Eagles, Phys. Rev. **186**, 456 (1969).

⁹ A. J. Leggett, in *Modern Trends in the Theory of Condensed Matter*, edited by A. Pekalski and R. Przystawa (Springer-Verlag, Berlin, 1980).

¹⁰ M. Randeria, in *Bose-Einstein Condensation*, edited by A. Griffin, D. Snoke, and S. Stringari (Cambridge University Press, 1995) Chap. 15.

¹¹ A. J. Leggett, *Quantum Liquids: Bose Condensation and Cooper Pairing in Condensed-Matter Systems* (Oxford University Press, 2006).

¹² C. A. Regal, M. Greiner, and D. S. Jin, Phys. Rev. Lett. **92**, 040403 (2004).

¹³ W. Ketterle and M. W. Zwierlein, (2008), arXiv:0801.2500.

¹⁴ S. Giorgini, L. P. Pitaevskii, and S. Stringari, Rev. Mod. Phys. **80**, 1215 (2008).

¹⁵ M. Gong, S. Tewari, and C. Zhang, ArXiv e-prints (2011), arXiv:1105.1796 [cond-mat.quant-gas].

- ¹⁶ H. Hu, L. Jiang, X.-J. Liu, and H. Pu, (2011), arXiv:1105.2488.
- ¹⁷ Z.-Q. Yu and H. Zhai, (2011), arXiv:1105.2250.
- ¹⁸ C. A. R. Sá de Melo, M. Randeria, and J. R. Engelbrecht, Phys. Rev. Lett. **71**, 3202 (1993).
- ¹⁹ P. Nozières and S. Schmitt-Rink, J. Low Temp. Phys. **59**, 195 (1985).
- ²⁰ E. J. Mueller, Phys. Rev. A **83**, 053623 (2011).
- ²¹ A more detailed classification of the non-Abelian gauge fields can be found in Ref. [6 and 7].
- ²² E. Braaten, M. Kusunoki, and D. Zhang, Ann. Phys. **323**, 1770 (2008).